EUROPEAN LABORATORY FOR PARTICLE PHYSICS
SL Division

CERN SL/92-40 (AP)

The design of betatron and momentum collimation systems

P.J. Bryant and E. Klein
SL Division, CERN

Abstract

Often a collimation system is required, not only to intercept particles that are outside prescribed betatron and momentum acceptances, but also to trap these particles with high efficiency. The motivation is to minimise background in physics detectors, to avoid quenching magnets in superconducting machines and to limit irradiation in transfer lines. After analysing the well-known one-dimensional betatron collimation insertion with zero dispersion, the problem of combining betatron and momentum collimation is solved. Optimum secondary collimator phases are found, the capture efficiency of the particles is shown to be independent of the amplitude of the dispersion function and the analysis is used to evaluate the effects of residual optics errors. The problem of uncontrolled scattering in the orthogonal plane is then solved by incorporating the earlier features into a two-dimensional system using specially shaped collimators. Once the orthogonal scattering is controlled the particles that escape the system have such small increases in amplitude that they can traverse the machine and be trapped on subsequent turns. The shaping of the collimators also enhances the impact parameter and improves the overall efficiency of the system.

Geneve, Switzerland
August 1992

1. Introduction

As beam energies and intensities increase, the need for very high efficiency collimation systems becomes more pressing in order to minimise background in physics detectors, to avoid quenching magnets in superconducting machines and to limit the irradiation of equipment in transfer lines. For these exacting tasks, the simple concept of placing two metal blocks either side of the beam to define an aperture is no longer sufficient. In the present paper, the problems of optimising the phases of secondary collimators, combining betatron and momentum collimation, evaluating the effect of optics errors, including the effects of energy loss in the primary collimator, controlling the scattering in the orthogonal plane and enhancing the impact parameter will be treated. Three types of system will be studied to illustrate these points;

- 1-dimensional system with zero dispersion (betatron collimation)
- 1-dimensional system with dispersion but zero bending (betatron & momentum collimation)
- 2-dimensional system with dispersion, but zero bending (betatron & momentum collimation).

2. Beam model

At a given azimuth in the machine, the beam is represented by a series of adjacent, phase-space ellipses, each of which represents a narrow momentum bite. The ellipse area equals the betatron emittance of the bite and the intensity can be indicated by shading. A beam with a dense core and a diffuse, large-emittance tail would appear as shown in Figure 1 with the ellipses spread out radially due to a finite local dispersion.

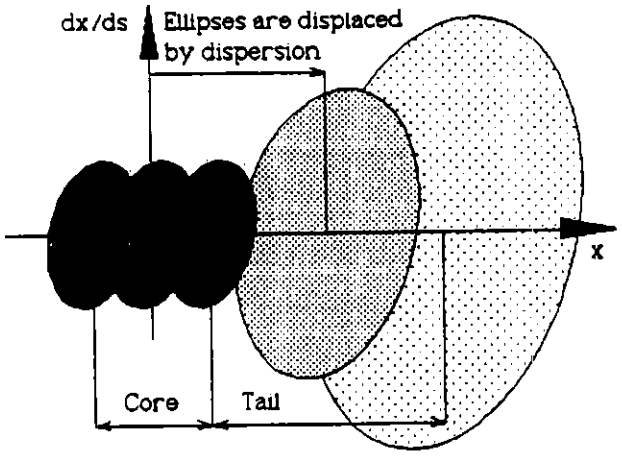

Figure 1 Beam with dense core and a low-momentum tail

Some further explanation is needed to explain the combination of the betatron and dispersion oscillations in phase space. The betatron oscillations are not closed over one turn and fill out an elliptical phase-space area. The dispersion oscillation, on the other hand, is a closed oscillation and, at a given azimuth in the machine, it defines only a point. The position coordinate of this point is the reason for the radial distribution of the ellipses in Figure 1. In a similar way, the ellipses should also be displaced parallel to the vertical axis to account for the longitudinal angle coordinate of the dispersion trajectory, but this has been omitted for simplicity, since a movement parallel to the image of a collimator in phase space will have no effect on the following argument.

However, it will be necessary to take this angle into account, when the ideal phase of the dispersion oscillation is specified for a combined collimation scheme.

It is now convenient to transform Figure 1 into normalised coordinates. The familiar parametric form of a betatron oscillation [1] is given below,

$$y(s) = F\sqrt{\beta(s)}\cos(\mu(s)+\phi) \tag{1}$$

where s is the distance along the central orbit, $y(s)$ is either of the transverse coordinates x or z, $\beta(s)$ is the betatron amplitude function, $\mu(s)$ is the betatron phase advance and F and ϕ are constants. The normalised phase-space coordinates are then defined as,

$$Y(\mu) = \left(\frac{y}{\sqrt{\beta}}\right) = F\cos(\mu+\phi) \tag{2}$$

and

$$\frac{dY}{d\mu} = \frac{d}{d\mu}\left(\frac{y}{\sqrt{\beta}}\right) = -F\sin(\mu+\phi) \tag{3}$$

where Y will be replaced by X or Z when appropriate. This transformation into normalised phase space reduces the betatron oscillations to simple harmonic motion. For later use, it is necessary to express $(dY/d\mu)$ in terms of more usual functions, that is,

$$\frac{dY}{d\mu} = \frac{d}{d\mu}\left(\frac{y}{\sqrt{\beta}}\right) = \frac{1}{\sqrt{\beta}}\frac{dy}{d\mu} - \frac{1}{2}\frac{y}{\beta^{3/2}}\frac{d\beta}{d\mu} \tag{4}$$

but

$$d\mu = \frac{1}{\beta}ds \quad \text{and} \quad \alpha = -\frac{1}{2}\frac{d\beta}{ds} \tag{5}$$

so that

$$\frac{dY}{d\mu} = \sqrt{\beta}\frac{dy}{ds} + \alpha\frac{y}{\sqrt{\beta}} \ . \tag{6}$$

In a bending-free region, the dispersion function $D(s)$ behaves exactly like a betatron oscillation. In analogy with the betatron case above, the dispersion oscillation and the corresponding normalised dispersion variables $(\chi, d\chi/d\mu)$ can then be defined as,

$$D(s) = D_0\sqrt{\beta(s)}\cos(\mu(s)+\varphi) \tag{7}$$

$$\chi = \frac{D}{\sqrt{\beta}} = D_0\cos(\mu+\varphi) \tag{8}$$

and

$$\frac{d\chi}{d\mu} = \sqrt{\beta}\frac{dD}{ds} + \alpha\frac{D}{\sqrt{\beta}} = -D_0\sin(\mu+\varphi) \ . \tag{9}$$

Figure 2 shows the transformation of Figure 1 to normalised phase space. The inclined axes of the ellipses map to the main axes and the ellipses are scaled to circles.

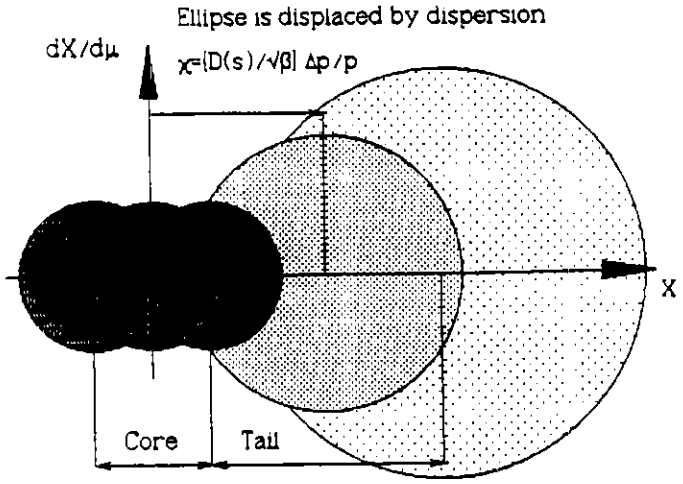

Figure 2 Normalised phase-space plot for a beam

It is important to note the similarity between betatron and dispersion oscillations and in particular, their complete equivalence in a bending-free region, since this is the underlying property that will make it possible to combine betatron and momentum collimation. This can be understood in general terms from the differential equations for particle motion in an alternating gradient lattice [1]. The motion due to a deviation in momentum from the nominal value is derived by adding a forcing term of the form $(1/\rho)(\Delta p/p)$ to the basic equation, but in a bending-free region $\rho = \infty$, the forcing term becomes zero and the equation reverts to its non-dispersive form. Thus in a bending-free region, a dispersion oscillation has exactly the same form and properties as a betatron oscillation (to first order).

3. Betatron collimation

For pure betatron collimation, the dispersion is made zero, so that all emittance ellipses coincide and all momenta are treated equally (see Figure 3). The principle for positioning the secondary collimators is thought to have been first given by Teng in [2]. It was independently developed in [3, 4] and has been applied in [5].

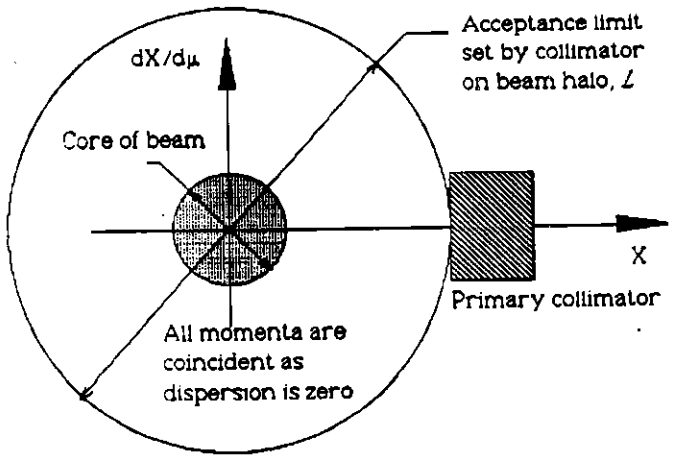

Figure 3 Action of primary collimator when dispersion is zero

As a first step, the scheme will be analysed in a way convenient for extending the general principle to the case of a combined betatron and momentum collimation insertion. The scheme uses a primary collimator (or scatterer) followed by two

secondary collimators that are optimised to intercept particles that are scattered by the primary block, but are still within the aperture of the vacuum pipe and thus pose a threat to the rest of the machine. Since the scheme is sited in a non-dispersive region any energy loss suffered by these scattered particles in the primary collimator is unimportant (to first order). The main features of the scheme are shown in Figure 4.

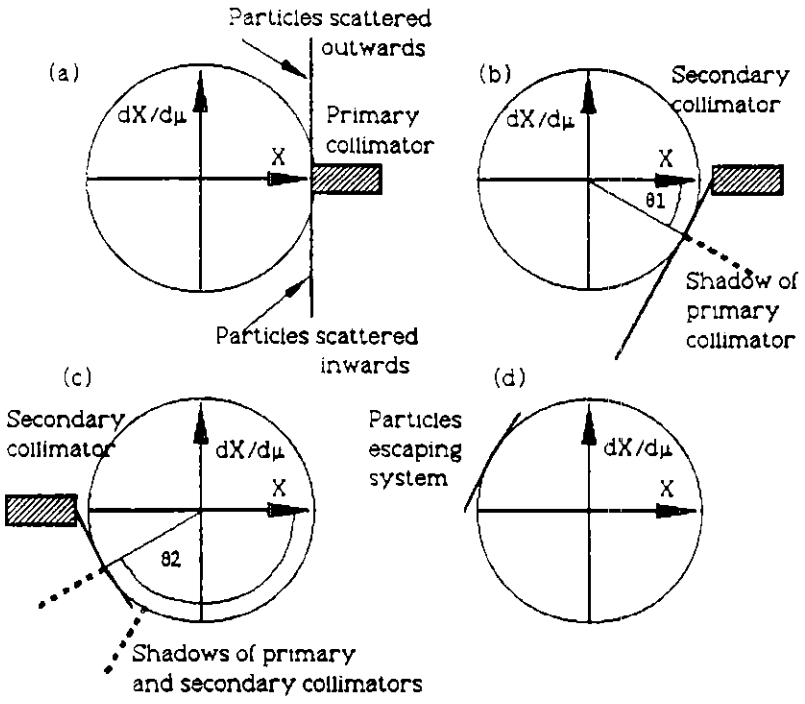

Figure 4 Main features of a single-stage collimation system

The optimum phase shifts between the primary collimator and its secondaries (see θ_1 & θ_2 in Figure 4) will correspond to the most efficient interception of the scattered tails. Consider Figure 5, in which the situation in Figure 4(b) is shown in more detail.

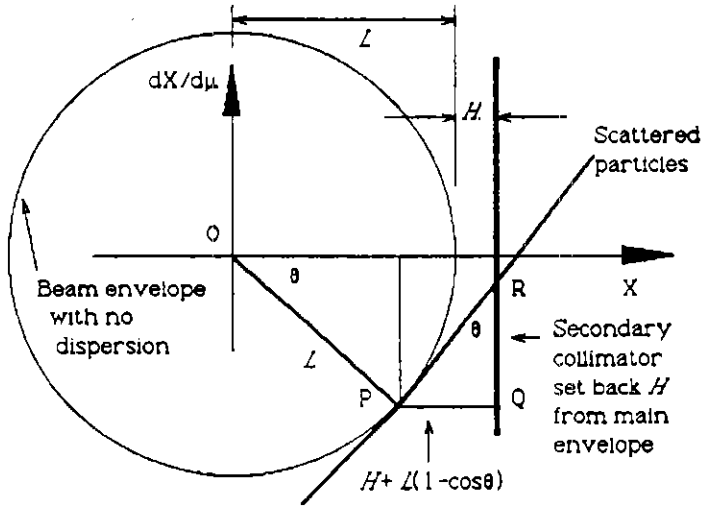

Figure 5 Action of secondary collimator [Detail of Fig 4(b)]

The scattered particles are spread out along a line at an angle θ equal to the betatron phase advance between the primary and secondary collimators. The secondary collimator is stepped back from the beam envelope to prevent it becoming a new

primary collimator. There is an optimum θ for which the length of the line PR of the locus of the scattered particles is a minimum. This optimum depends upon the radius of the beam envelope, which equals the half-aperture of the primary collimator L (normalised) and the step back H (normalised).

By geometry,
$$\mathrm{PR} = \frac{[H + L(1-\cos\theta)]}{\sin\theta} \tag{10A}$$

and after rearranging
$$\mathrm{PR} = L\tan\left(\frac{\theta}{2}\right) + \frac{H}{\sin\theta} \; . \tag{10B}$$

As a quick check it can be seen that PR$\rightarrow\infty$ when θ=0 and PR=L+H when θ=90^0. The minimum of PR is found by differentiation of (10B),

$$\frac{\mathrm{d\,PR}}{\mathrm{d}\theta} = \frac{L}{2}\sec^2\left(\frac{\theta}{2}\right) - \frac{H\cos\theta}{\sin^2\theta} = 0 \tag{11}$$

which yields the optimum phase advance θ_1 of the first secondary collimator as,

$$\theta_1 = 2\sin^{-1}\sqrt{\left[\frac{1}{2}\left(\frac{H}{L+H}\right)\right]} \; . \tag{12}$$

By inspection, it can be seen that the phase advance θ_2 of the second secondary collimator will be 180^0-θ_1. Equation (12) has been evaluated numerically in Table 1.

It can be seen from Figure 5 that the particles escaping the system are contained within a normalised acceptance circle of radius, $\mathrm{OR}^2 = \mathrm{PR}^2 + L^2$ and a little further manipulation will show that at the optimum phase advance θ_1, the point R moves onto the real axis, so that OR is a minimum and is simply given by,

$$\mathrm{OR}_{\min} = L + H \; . \tag{13}$$

If this is still within the acceptance of the rest of the machine, then the escaping particles will be trapped on the primary collimator some turns later and the overall efficiency is improved. Table 1 includes the normalised acceptance of the escaping particles in the plane of collimation.

Table 1 Typical parameters for a single-stage collimation scheme

H/L	0	0.05	0.1	0.15	0.2	0.25
θ_1 [degree]	0	17.8	24.6	29.6	33.6	36.9
$\mathrm{OR}_{\min}$*	L	1.05L	1.1L	1.15L	1.2L	1.25L

There is a complication in the above model. The primary collimator also scatters the escaping particles in the orthogonal plane and, in many cases, the increase in

* The limit acceptance OR of the escaping particles is expressed in units of L which is the normalised half-aperture of the primary collimator. A practical unit for L and OR that is used widely for apertures would be a standard deviation of the nominal beam emittance.

amplitude will be far larger than in the plane of collimation causing the particles to be lost elsewhere in the machine. This problem is described in [6] and a solution is proposed in Section 7.

4. Combined betatron and momentum collimation in a bending-free region with dispersion

In the presence of dispersion, the primary collimator will no longer cut the betatron emittance ellipses for all momenta to the same degree. The primary collimator will impose a different acceptance ellipse for each momentum as shown in Figure 6. This figure is the sequel to Figure 4 and shows the beam at the exit of the collimator.

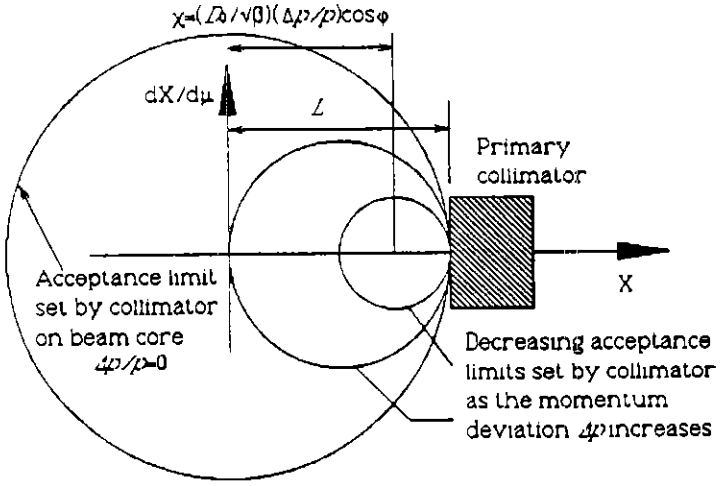

Figure 6 Action of primary collimator when dispersion is non-zero

If A is defined as the normalised amplitude of the betatron acceptance ellipse for a given momentum deviation, then the primary collimator will set this limiting amplitude according to,

$$A = L - \frac{D_0}{\sqrt{\beta}} \frac{\Delta p}{p} \cos\varphi \qquad (14)$$

where L is the normalised half-aperture of the primary collimator and μ is taken as zero at the primary collimator so that φ gives the phase of the dispersion oscillation.

At a betatron phase θ later, the beam will pass the first of the two secondary collimators that are set back from the beam envelope by a distance H. It is assumed that the beam envelope is defined by the acceptance ellipse set by the primary collimator on the core beam of nominal momentum and this assumption will be justified later. Upon arrival at the secondary collimator, all ellipses will have rotated by θ, but those with a non-zero momentum deviation will also have been moved radially by the dispersion oscillation. This is illustrated in Figure 7 for an individual off-momentum ellipse that is moved towards the central orbit and away from the collimator by the dispersion oscillation. For the off-momentum ellipse the scattered particles lie along the line PR at the time the secondary collimator is passed. The length of the line PR represents the particles that escape the collimator and is therefore a measure of the system's efficiency. Clearly, an uncontrolled dispersion is potentially very dangerous for the overall efficiency of the system.

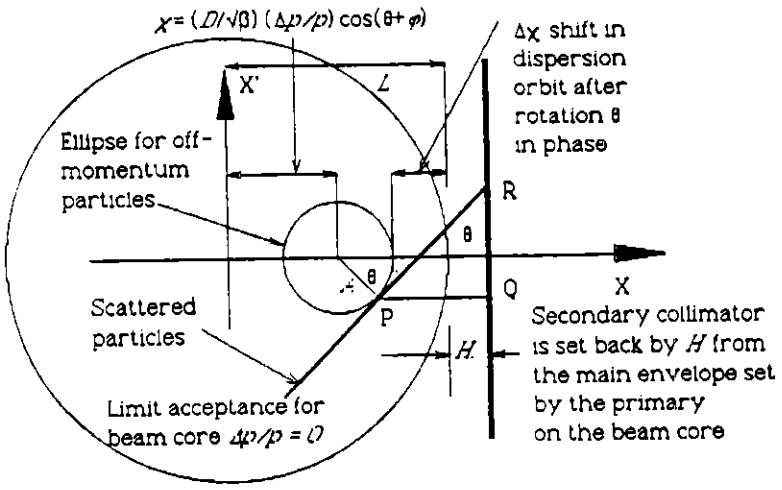

Figure 7 Action of a secondary collimator with dispersion

From the geometry of Figure 7,

$$PR = PQ / \sin\theta = [H + \Delta\chi + A(1-\cos\theta)] / \sin\theta \qquad (15)$$

where $\Delta\chi$ is the normalised movement of the dispersion orbit and is given by,

$$\Delta\chi = \frac{D_0}{\sqrt{\beta}} \frac{\Delta p}{p} [\cos\varphi - \cos(\varphi+\theta)] \qquad (16)$$

If the phase of the normalised dispersion oscillation is chosen to be zero at the primary collimator (i.e. φ=0), then

$$\Delta\chi = \frac{D_0}{\sqrt{\beta}} \frac{\Delta p}{p} [1-\cos\theta] \qquad (17)$$

The length of PR given in (15) can now be written as,

$$PR = [H + \frac{D_0}{\sqrt{\beta}} \frac{\Delta p}{p} (1-\cos\theta) + A(1-\cos\theta)] / \sin\theta \qquad (18)$$

but A has already been determined in (14), so by substitution into (18),

$$PR = \frac{[H + L(1-\cos\theta)]}{\sin\theta} . \qquad (19)$$

This is exactly the same result as was obtained in (10A) for the non-dispersion case and consequently the optimum phase advances for the secondary collimators remain unchanged. In theory, chromatic effects will adversely affect the above by making θ a function of momentum, but in practice, a collimation insertion will have less than 180^0 phase advance and it is unlikely that sextupoles will be included, so these complications can be ignored.

Three important statements can now be made :

(i) When the normalised dispersion has its peak at the primary collimator, all momenta are treated equally as in the non-dispersion case with the standard phases for the secondary collimators.

The condition for the normalised dispersion oscillation to have its peak at the primary collimator can be found by equating (9) to zero,

$$\frac{d\chi}{d\mu} = \sqrt{\beta}\frac{dD}{ds} + \alpha\frac{D}{\sqrt{\beta}} = 0 \qquad (20)$$

to give

the collimation condition , $$\frac{1}{D}\frac{dD}{ds} = -\frac{\alpha}{\beta} \quad \text{at the primary.} \qquad (21)$$

(ii) As far as the efficiency (i.e. capture of particles) is concerned, there is no preferred value for the dispersion amplitude D_0.

(iii) Furthermore, the slope of the beam envelope at the location of the primary collimator is independent of the momentum (as shown in Appendix) thus the primary collimator can be aligned longitudinally for all momenta at maximum efficiency.

Thus a combined betatron and momentum collimation scheme requires the above condition (21) to be fulfilled at the primary collimator, to ensure that the dispersion and betatron oscillations have their correct phases. In the past, when schemes have been installed in dispersive regions, they have either been positioned by other criteria as in the ISR [7], or by simulations as in LEP [8].

5. Energy loss in the primary collimator

The above analyses have considered scattered particles starting from the exit of the primary collimator. Among these particles, there will be a spectrum of energy losses that may be very large or very small depending upon the beam energy and the material and thickness of the primary collimator. In the case of the betatron collimation system, the insertion is in a non-dispersive region and is therefore insensitive to these energy changes. This is also true of the combined betatron and momentum insertion described above, but it is worth briefly considering this point.

All the phase-space diagrams shown so far have been drawn for positive momentum deviations, but a collimator on the side with negative momentum deviations would work in exactly the same fashion. It is only when the concept of an energy loss in the primary collimator is introduced that some asymmetry occurs. This is illustrated in Figure 8. An energy loss always moves the equilibrium orbit of a particle to the left in the diagram. For particles with a large positive momentum deviation, a small loss in momentum makes no significant difference and there is no way of distinguishing such particles in Figure 6 for example. For a particle with a large negative momentum deviation, an energy loss can cause its equilibrium orbit to move outside the main beam envelope and the betatron phase (of the zero scattered reference particle) is then set to increase its negative excursion. At first sight, this appears to be a problem, but in fact it is exactly what is required. The large negative momentum deviation moves the particle rapidly towards central orbit as the dispersion oscillation reduces in amplitude and the betatron oscillation moves away from central orbit by enough to ensure the correct positioning of the particle at the next secondary collimator.

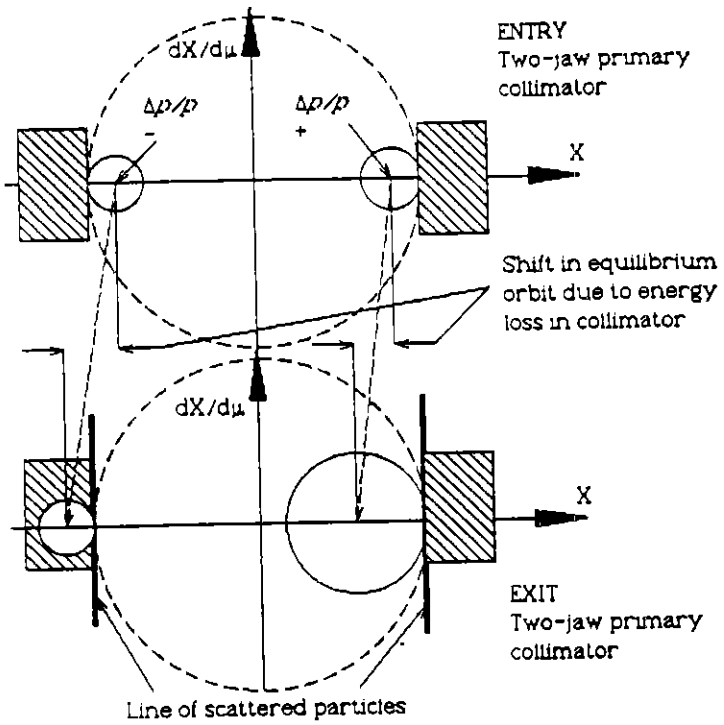

Figure 8 Effect of energy loss in the primary collimator

6. Effect of residual dispersion errors

The principal risk when operating a collimation insertion is that of making the stepback of either of the secondary collimators a 'stepforward' (i.e. $H \leq 0$). This would make the secondary an 'unprotected' primary from which scattered particles would go straight into the machine. This is a potentially dangerous situation, especially for a superconducting machine and for physics detectors. Unfortunately, 'trial-and-error' adjustment will be prone to making this mistake, since the efficiency of the insertion improves as H is decreased and then jumps discontinuously (when $H = 0$) to the catastrophic situation described above. Prediction of the point at which this change occurs will be made uncertain by residual errors in the optics.

Thus, any error in the movement of an emittance ellipse due to the dispersion oscillation must always be less than the collimator stepback. However, the stepback is a variable parameter and, in practice, a compromise would be sought between this and the mechanical limitations on the collimator adjustment One compromise would be to make the minimum stepback (H_{min} normalised) equal to the smallest collimator movement. The movement of an emittance ellipse is given by (16). The residual errors ΔD and $\Delta\varphi$ can be added in a straightforward way and a limit criterion can be constructed as in (22). The limit should be evaluated for the largest $\Delta p/p$ expected.

$$0 \leq H_{min} - \left| \frac{(D_0 + \Delta D)}{\sqrt{\beta}} \left[\cos\Delta\varphi - \cos(\Delta\varphi + \theta_1)\right] - \frac{D_0}{\sqrt{\beta}} \left[1 - \cos\theta_1\right] \right| \left(\frac{\Delta p}{p}\right)_{max} . \quad (22)$$

For a pure betatron collimation insertion, $D_0 = 0$ and $\Delta\varphi$ may have any phase from 0 to 2π. In this case, the remaining cosine terms can be shown to have an amplitude not greater than $\sqrt{2(1-\cos\theta_1)}$, so that (22) reduces to first order to,

$$h_{min} \geq \left|\Delta D\sqrt{2(1-\cos\theta_1)}\right| \left(\Delta p/p\right)_{max} . \tag{23}$$

Note that the normalised stepback H_{min} has been changed to the real space value h_{min} which is more useful in this case.

For a combined betatron and momentum collimation insertion, there will be a dominate dispersion vector and, unlike the previous case, $\Delta\phi$ will be small, so that $\cos(\Delta\varphi) \rightarrow 1$, $\sin(\Delta\varphi) \rightarrow \Delta\phi$ and (22) reduces to first order to,

$$h_{min} \geq \left|\Delta D(1-\cos\theta_1) + D_0\Delta\varphi\sin\theta_1\right| \left(\Delta p/p\right)_{max} . \tag{24}$$

7. Two-dimensional collimator systems

The main drawback of the systems described so far is the lack of control of the scattering in the orthogonal plane. This can be solved by working in two-dimensions with a shaped primary collimator.

7.1 More about the beam model

In phase space the beam particles follow ellipses or circles, whereas in real space they sweep over rectangular areas as shown in Figure 9(a). The motion is close to being simple harmonic in the two planes so that the probability density of finding a particle in its rectangle is highest in the corners and lowest at the centre. This assumes that the particles are not locked in resonances, but have non-rational tunes. The largest rectangles that can exist within the aperture will just touch the aperture limit. In this way, a beam takes up the shape of an aperture limit and fills the space. The fact that beams always appear dense at the centre and elliptical, or circular, in shape may appear to refute this, but this effect is due to the very large number of particles within a normal beam and the way their 'rectangles' are distributed by size and aspect ratio.

This model will be used to compare the scattering actions of a collimator that is parallel to one of the betatron oscillation axes to one that is inclined. It will also give an intuitive indication of the results obtained in [6] for the impact parameter.

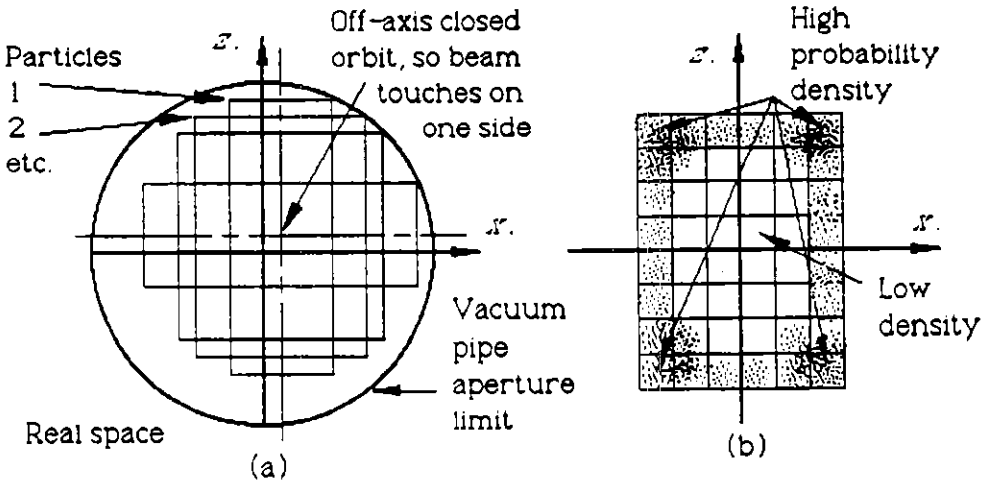

Figure 9 Beam model in real space. (a) Some particles with an off-axis closed orbit at the aperture limit. (b) Probability density swept out by one particle (schematic).

7.2 Scattering in the orthogonal plane [6]

First consider scattering in an upright collimator aligned with the vertical betatron oscillations as shown in Figure 10. When a particle hits the collimator it is scattered without any preferential direction, so it is necessary to consider scattering in the plane of collimation and in the orthogonal plane.

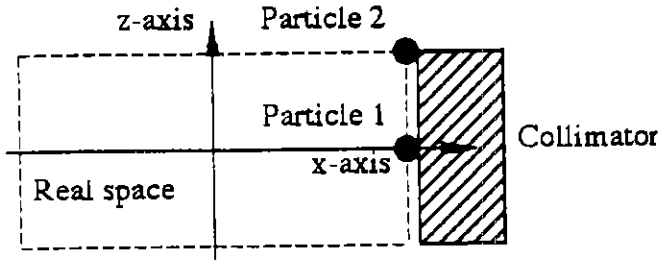

Figure 10 Upright collimator against a beam in real space

In Figure 1, particle **1** on the x-axis is at the peak of its horizontal oscillation and at the centre of its vertical oscillation, while particle **2** is at the peak of both its horizontal and vertical oscillations. For argument's sake, it is assumed that the scattering angles are equal in both planes and for both particles. The normalised phase-space plots then appear as shown in Figure 11.

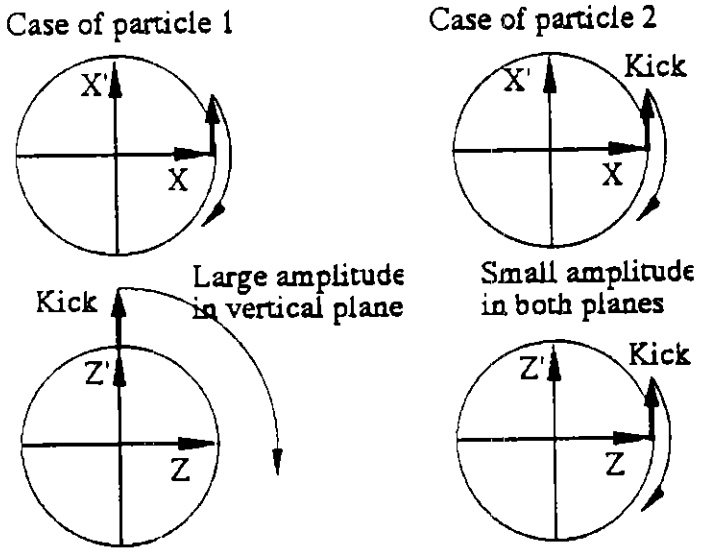

Figure 11 Normalised phase-space plots for scattered particles

Horizontally the situation is equal for the two particles. The scattering causes a shift parallel to the X'-axis and the particle moves in phase but little in amplitude. This is the case described in Section 3. In the vertical plane, particle **2** is also at the maximum of its vertical oscillation and its phase-space diagram is a repeat of the horizontal plane. Particle **1** is different, however, and the kick adds fully to its amplitude. In Section 3, it is explained that particles with very small horizontal scattering will escape the secondary collimators. These escaping particles will have a distribution of vertical amplitudes similar to particle **1** and are likely to be lost later in the machine. This is the problem of uncontrolled scattering in the orthogonal plane.

There is an advantage in minimising the particles of type **1**, since unlike particles of type **2**, their enhanced amplitude gives them little chance of surviving a full turn of the machine and being caught by the collimator system some time later. A collimator with an inclined, or curved face, such as the circular aperture limit shown in Figure 9(a)

will preferentially select the particles that are at the peaks of both their oscillations and will ensure controlled scattering in both planes.

7.3 Optics and design of a 2-dimensional collimator system

The design of a 2-dimensional system is made easy by choosing equal phase advances with distance in both planes and equal betatron amplitudes. This can be achieved by adopting a low-β optics as shown in Figure 12. This has already been proposed for LHC in Ref.[4] for pure betatron collimation with two 1-dimensional systems.

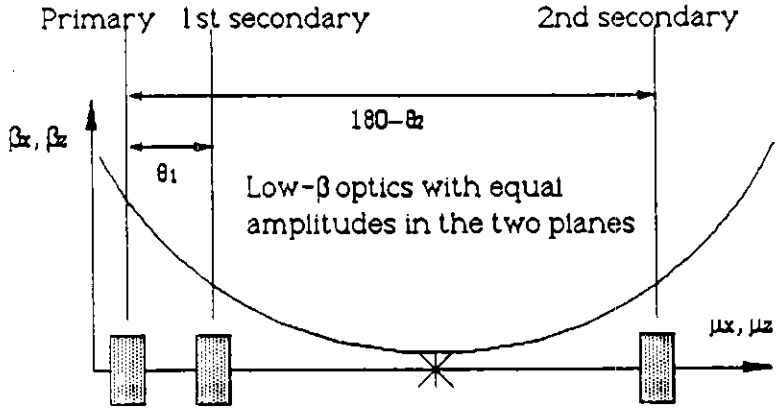

Figure 12 Optics for a 2-dimensional collimator system

Into this optics place a primary collimator with a circular aperture L followed by a secondary collimator with a circular aperture $L+H$. The shape of the primary collimator aperture will preferentially select particles at the maxima of their oscillations and a typical particle with a momentum deviation is shown in Figure 13. In the secondary collimator, the position of the unscattered particle is shown with a schematic circle indicating the possible scattering.

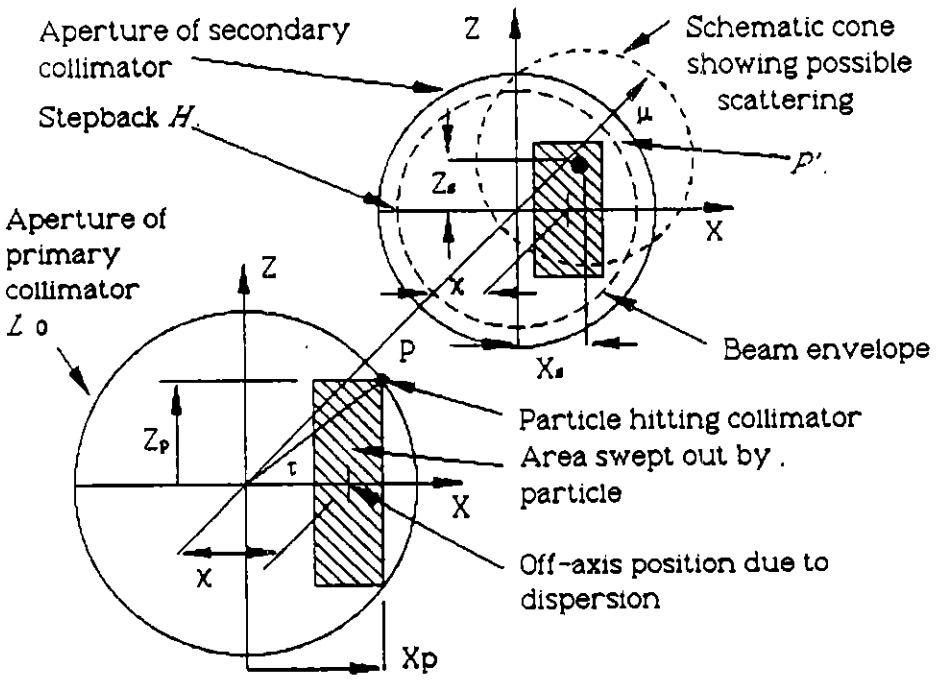

Figure 13 Action of primary and secondary collimators in a two-dimensional scheme

The beam envelope at P maps to P', which in real space scales with $\sqrt{\beta_x}$ and $\sqrt{\beta_z}$ but is invariant in normalised coordinates. The secondary collimator is placed outside this point as shown and its exact shape will be derived below. The particle at P with angle τ has been limited to the horizontal and vertical apertures,

$$X_p = L_0 \cos\tau \quad \text{and} \quad Z_p = L_0 \sin\tau \tag{25}$$

where L_0 is the normalised radius of the primary aperture and τ can assume any value from $0 \rightarrow \pi/2$. This is equivalent to placing normal collimators at X_p and Z_p in the usual way. The X and Z motions between the collimators can be treated independently and correspond to all the previous results with L replaced by (25) Since the betatron amplitudes have been chosen as equal in the two planes both the horizontal and vertical motions require the secondary collimator at the same place. Figure 7 then applies in both planes, except that in the vertical plane the dispersion is zero and it degenerates to Figure 5. Now place hypothetical collimators of the normal type at the coordinates of the point R in real space. It was shown in Section 3 in (13) that the point R would be at the normalised coordinates $(L+H)$ in each plane. If now the point P is moved to anywhere on the aperture limit of the primary collimator the locus of R will describe the profile of the secondary collimator. With the use of (25),

$$\begin{aligned} OR_{min}^{\ 2} &= (L+H)_{HORIZ}^{\ 2} + (L+H)_{VERT}^{\ 2} \\ &= (L_0 \cos\tau + H)^2 + (L_0 \sin\tau + H)^2 \\ &= L_0^{\ 2} + 2H^2 + 2\sqrt{2} L_0 H \sin(\tau + \pi/4) \end{aligned} \tag{26}$$

The profile given by (26) for $0 \le \tau \le \pi/2$ should be applied to each quadrant. When $\tau=0$ or $\pi/2$, $OR_{min}=L_0+H$ (to first order in H/L), which is the normal 1-dimensional situation. When $\tau = \pi/4$, $OR_{min}=L+\sqrt{2}H$. Thus, there is a small correction to be made to the surface of the secondary collimators that increases the standard stepback H on the X- and Z- axes to $\sqrt{2}H$ on the 45^0 lines.

Furthermore, if L_0 is made a function of τ then (26) can be used to find the profile of the secondary for <u>any shape of primary</u>.

$$OR_{min} \approx [L_0(\tau) + H]\left\{1 - [H / L_0(\tau)][1 - \sqrt{2}\sin(\tau + \pi/4)]\right\} \tag{27}$$

All the results of the previous sections can now be applied directly in the 2-dimensional case. The optimum secondary collimator phases are equal in the two planes and are given by (12). If dispersion is required in one plane then the condition (21) must be applied at the primary collimator. Finally, the profile of the secondary is given by (27) where $L_0(\tau)$ is the profile of the primary.

The above scheme has the major advantage over the preceding schemes that any particle that escapes the system will be contained within the normalised aperture $OR_{min} = L+H$ (see Section 3 and Table 1) <u>in both planes</u>. If therefore, the primary collimator is set so that the machine acceptance is greater than, or equal to, $L+H$ in both planes, then the efficiency of the insertion can theoretically reach 100 percent assuming that all particles that hit a secondary collimator are absorbed. More collimators could be added to intercept even these particles, but there would be a penalty to pay in the time needed to set up and optimise the system.

7.4 2-dimensional collimator design

In an unprotected machine, the circular vacuum chamber would act somewhat like the 2-dimensional collimator described above. Thus, for chamber protection, circular primary and secondary collimators would appear to be an ideal choice, which would also be insensitive to coupling as mentioned in [6]. Inclined collimators set at 45^0 would also be possible. In practice, a hybrid of these two possibilities is the simplest to build as shown in Figure 14.

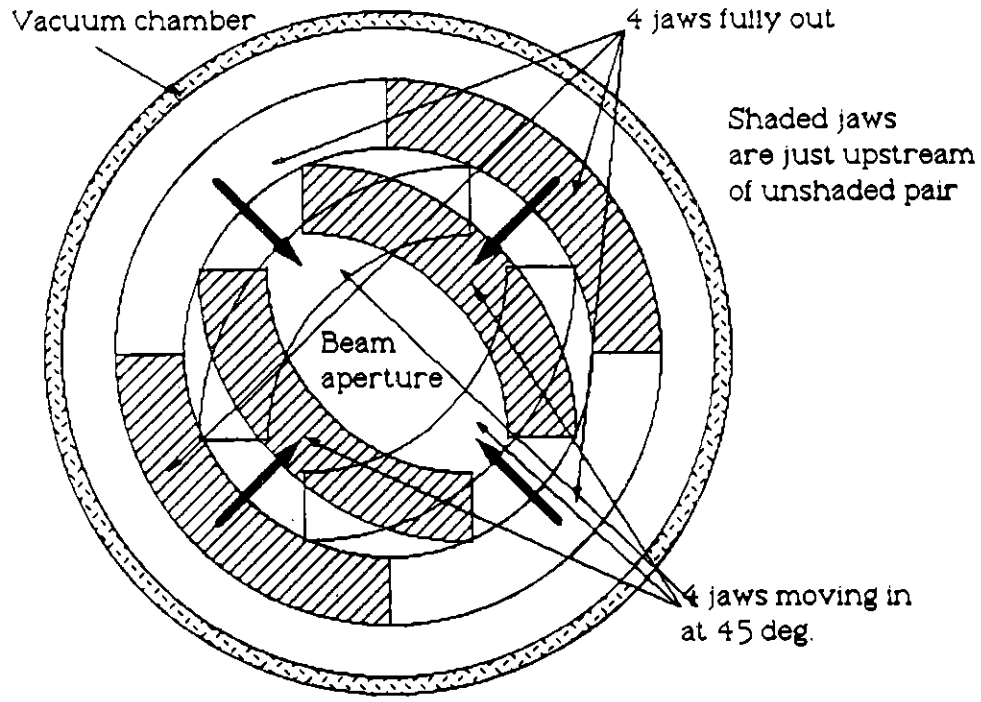

Figure 14 4-jaw circular collimator

7.5 Enhancement of the impact parameter

Figure 9(b) gives a schematic indication of the probability density to find a particle in real space. An upright collimator aligned with one of the betatron oscillations will integrate over the probabilities along one full side of the rectangle, whereas an inclined collimator can only intercept the corner of the rectangle. It is expected therefore that more turns are needed on average to hit an inclined collimator than an upright one. If the beam is slowly expanding, or the collimator advancing, then the extra turns should enhance the impact parameter. This is explored in more detail in [6].

8. Conclusions

The design parameters for a 1- and 2- dimensional collimation systems have been derived and it has been shown how to build a 2-dimensional system with very high efficiency. The points optimised or enhanced are:

- The impact parameter on the primary collimator and its alignment,
- The stepback H of the secondary collimators and the collimator phases,
- The way in which dispersion is accommodated and
- The control of the scattering by the primary collimator in the plane orthogonal to the plane of collimation.

An extremely useful addition to a collimation system is one or more dipole bends with strategically placed absorbers. Particles with large momentum errors and incorrect charge to mass ratios can then be swept out of the beam and captured at a precise location rather than throughout the insertion. The dipoles, however, introduce dispersion and, unless they can be made self-compensating in some way, they will introduce an error in the optimisation of the secondary collimators. This applies equally to the pure betatron and the combined betatron and momentum collimation insertions. The error can probably be made acceptably small, especially in large high-energy machines. The limits given in Section 6 help to define what is acceptable and what is not.

The combined collimation insertion cuts a profile onto the beam. The nominal momentum has the largest emittance and the extreme momentum deviations have smaller, or zero, emittance. In the case of a machine protection insertion for a collider such as LHC, the collimators would need to be the momentum and betatron aperture limit of the machine and it would be natural to make D_0 at the primary collimator a little larger than in the arcs. The parameters could be arranged so that approximately six standard deviations of the nominal momentum spread in the rf bucket, or six standard deviations of the nominal emittance (or any combination) would be needed to reach the primary collimator. Since the stored beam is trapped in rf buckets with a relatively narrow momentum spread the 'profile' effect would not be important and would in any case only mimic the effect of the vacuum chamber if that were the limiting aperture.

9. Acknowledgments

The authors would like to thank T. Risselada for his comments and M. Bassetti and J. Gareyte for helpful discussions.

10. References

1. K. Steffen, "Basic course on accelerator optics", CERN 85-19, 25-63.
2. L.C. Teng, "Design concepts for the beam scaper system of the main ring", Int. Report. Fermilab, FN-196/0400, (17 Oct. 1969).
3. J.B. Jeanneret, "Phase difference between collimators in a collider", SL/EA/Note 90-01.
4. The LHC Study Group, "Design study of the Large Hadron Collider (LHC)", CERN 91-03, 115-25.
5. M. Seidel, "The HERA-p collimation system and first experience with a single collimator", HEACC 92, Hamburg,1992, (to be published).
6. P.J. Bryant, "Some advantages of inclined collimators", CERN SL/92-24 (AP).
7. T. Risselada, R. Jung, D. Neet, H. O'Hanlon, L. Vos, "The ISR collimator system", 1979 Part. Accel. Conf., San Francisco, NS-26, No. 3, 4131-3.
8. G. von Holtey, "Electron beam collimation at LEP energies", Proc. 1987 IEEE Part. Accel. Conf., Washington, (IEEE Cat. No. 87CH2387-9), Vol. 2, 1252-4.

11 Appendix A
Slope of the beam envelope at the primary collimator

The following has been pointed out by Thys Risselada. When the collimation condition (21) is satisfied at the primary collimator, the slope of the beam envelope is independent of the momentum. This means that the alignment of the collimator with the beam envelope is valid for all momenta and consequently its interception efficiency is also independent of the momentum.

The collimator must be aligned longitudinally with the local beam envelope. The amplitude of this envelope at the entry to the collimator is given by the contributions of two terms, one coming from the betatron oscillation envelope, the other coming from the dispersion oscillation, which is maximum at this point.

$$x_{\text{collimator}} = F\sqrt{\beta} + D\ \ \Delta p / p \tag{1A}$$

After differentiation,

$$\begin{aligned} x'_{\text{collimator}} &= \frac{1}{2}\frac{F\sqrt{\beta}}{\beta}\frac{d\beta}{ds} + \frac{dD}{ds}\frac{\Delta p}{p} \\ &= -\frac{\alpha F\sqrt{\beta}}{\beta} + \frac{dD}{ds}\frac{\Delta p}{p} \end{aligned} \tag{2A}$$

Taking into account the collimation relation (21), $\frac{dD}{ds} = -\frac{\alpha}{\beta}D$

one obtains with (1A)

$$x'_{\text{collimator}} = -\frac{\alpha F\sqrt{\beta}}{\beta} + \left(-\frac{\alpha}{\beta}D\right)\frac{\Delta p}{p} = -\frac{\alpha}{\beta}x_{\text{collimator}} \tag{3A}$$

which is independent of momentum.